Available online at www.sciencedirect.com
SCIENCE DIRECT®
ELSEVIER
Cryogenics 43 (2003) 589–596
Cryogenics
www.elsevier.com/locate/cryogenics

Cryogenic cooling system of HTS transformers by natural convection of subcooled liquid nitrogen

Ho-Myung Chang [a,*,1], Yeon Suk Choi [a], Steven W. Van Sciver [a], Kyeong Dal Choi [b]

[a] National High Magnetic Field Laboratory, Tallahassee, FL 32310, USA
[b] Korea Polytechnic University, Shihung-Shi, Kyonggi-Do 429-793, South Korea

Abstract

Heat transfer analysis on a newly proposed cryogenic cooling system is performed for HTS transformers to be operated at 63–66 K. In the proposed system, HTS pancake windings are immersed in a liquid nitrogen bath where the liquid is cooled simply by colder copper sheets vertically extended from the coldhead of a cryocooler. Liquid nitrogen in the gap between the windings and the copper sheets develops a circulating flow by buoyancy force in subcooled state. The heat transfer coefficient for natural convection is estimated from the existing engineering correlations, and then the axial temperature distributions are calculated analytically and numerically with taking into account the distributed AC loss in the windings and the thermal radiation on the walls of liquid-vessel. The calculation results show that the warm end of the HTS windings can be maintained at only 2–3 K above the freezing temperature of nitrogen, with acceptable values for the height of HTS windings and the thickness of copper sheets. It is concluded that the cooling by natural convection of subcooled liquid nitrogen can be an excellent option for compactness, efficiency, and reliability of HTS transformers.

Keywords: Nitrogen (A); Heat transfer (C); Cryostats (E); Transformers (E)

1. Introduction

HTS transformers have a variety of potential advantages over conventional units in compactness, efficiency, fire safety, and over-load operation. One of the key techniques to realize these advantages in practice is the cryogenic design, as the cooling system of HTS windings determines to a large extent the size, the weight, the power consumption, and even the reliability of the entire transformer unit. After the initial efforts to successfully demonstrate the feasibility of HTS transformers [1], a few different configurations of cryogenic system have been designed and tested worldwide for the past several years.

Japanese group led by Kyushu University [2,3] contained the HTS windings in a main GFRP cryostat filled with subcooled liquid nitrogen at around 65 K, and located an iron core through room-temperature bore of the cryostat. The subcooled liquid is continuously chilled by two sets of GM cryocoolers in a secondary cryostat and circulated through transfer lines to the main cryostat by a pump, as shown in Fig. 1(a). The US team under the Department of Energy SPI (Superconductivity Partnership Initiative) agreement [4] has pursued a completely different cooling design. In order to avoid the expensive composite cryostat, they placed both the windings and the iron core in vacuum tank. The HTS windings were maintained at around 30 K by the circulation of helium gas chilled by a GM cryocooler, and the radiation shields were cooled at 77 K by liquid nitrogen and another cryocooler. Fig. 1(b) illustrates a simplified schematic of their cooling module. Siemens in Germany [5] has developed the HTS transformers for railway applications. As geometric constraint and compactness are more significant than efficiency in the on-board transformers, the whole core-and-coil assembly was cooled at around 67 K with subcooled liquid nitrogen. A huge capacity of Stirling cooler was employed for a laboratory test to supply the subcooled liquid through transfer tubes, as shown in Fig. 1(c).

* Corresponding author. Tel.: +1-850-644-0858; fax: +1-850-644-0867.
E-mail address: chang@magnet.fsu.edu (H.-M. Chang).
[1] On leave from Hong Ik University, Seoul, Korea.

0011-2275/$ - see front matter © 2003 Elsevier Ltd. All rights reserved.
doi:10.1016/S0011-2275(03)00168-1

Nomenclature

A	axial cross-sectional area [m^2]
F	radiation shape factor
g	gravitational acceleration [m/s^2]
H	height of HTS pancake windings [m]
h	convective heat transfer coefficient [W/m^2 K]
h_c	contact heat transfer coefficient [W/m^2 K]
k	thermal conductivity [W/m K]
L	horizontal distance between vertical surfaces [m]
Nu	Nusselt number, $h \cdot L/k$
P	perimeter of convection heat transfer [m]
Q_{ac}	AC loss in HTS windings [W]
Q'_r	thermal radiation per unit axial length [W/m]
Ra	Rayleigh number, $g\beta \cdot \Delta T \cdot L^3/(\nu \cdot \alpha)$
T	temperature [K]
z	axial distance from bottom of HTS winding [m]

Greek letters

α	thermal diffusivity [m^2/s]
β	thermal expansion coefficient [1/K]
δ_C	thickness of copper sheet [mm]
ε	emissivity of surface
ν	kinematic viscosity [m^2/s]
σ	Stefan–Boltzmann constant [W/m^{2}K^4]

Subscripts

C	copper sheet
G	GFRP wall of liquid-nitrogen vessel
H	HTS pancake winding
R	room-temperature wall

A Korea–USA collaborative research involving the cryogenics for HTS transformers is underway at the National High Magnetic Field Laboratory. The objective of this project is the design of cryogenic cooling systems for the recently started HTS transformer programs in both countries. In Korea, the CAST (Center for Applied Superconductivity Technology) launched a 10-year project at Korea Polytechnic University (KPU) [6] as a part of the 21st Century Frontier R&D Program. In the US, the CAPS (Center for Advanced Power Systems) initiated another HTS transformer project [7] as a part of the ONR (Office of Naval Research) All-Electric Ship Program. As a beginning step, we have presented a thermodynamic optimization of the operating temperature, aiming simultaneously at compactness and efficiency of HTS transformers [8,9]. In accordance with the results of the preliminary study, we try to explore a continuous cryocooling system at 63–66 K, which will be applied to the prototype of 1 MVA single-phase transformer at KPU. Some of the given parameters for the KPU transformer are listed in Table 1. The main purpose of this paper is to propose a new cryogenic design for the specific HTS transformer and then evaluate its thermal characteristics by performing a relevant heat transfer analysis.

Fig. 2 is a schematic representation of our proposed cooling system. The HTS pancake windings are immersed in a liquid nitrogen bath where the liquid is cooled simply by cold copper sheets vertically extended from the coldhead of a closed-cycle cryocooler located above. Liquid nitrogen in the gap between the windings and the copper sheets will develop a circulating flow by buoyancy force in subcooled state close to the normal freezing point as indicated on a phase diagram in Fig. 3. Nitrogen functions as a heat transfer medium and an electrical insulating fluid at the same time. Since no circulating pump or transfer line is necessary, the proposed cooling by natural convection has great advantages in all aspects of compactness, efficiency, and reliability, over the forced-flow cooling of the previous systems [2–5]. On the other hand, the heat transfer coefficient in natural convection is generally much smaller than in forced convection, which may cause an excessively high temperature of the HTS windings or diminish the essential merits of the low- temperature operation below 77 K. Thus, the heat transfer analysis to accurately predict the temperature distribution in the cooling system is crucial in confirming the feasibility of our proposed design.

2. Natural convection in vertical cavity

As the radial gap filled with liquid is much smaller than the radius of the windings in the cooling system, we may well consider the problem as natural convection in a rectangular cavity, where a vertical wall is heated and the other vertical wall is cooled. A number of experimental and theoretical studies have been performed on this subject, suggesting useful correlations in a standard form [10,11],

$$Nu = \frac{h \cdot L}{k} = f\left(Ra, \frac{\nu}{\alpha}, \frac{H}{L}\right) \tag{1}$$

where Nu is the Nusselt number composed of the heat transfer coefficient, h, the thermal conductivity of fluid, k, and the horizontal distance between the vertical surfaces, L, and the Rayleigh number is defined as

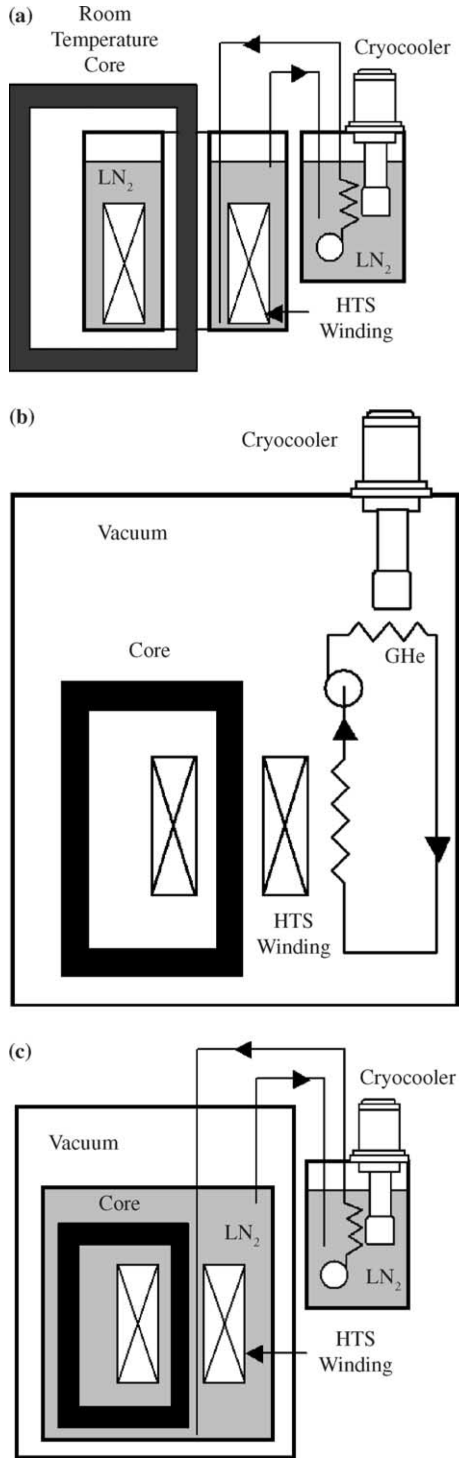

Fig. 1. Schematic configurations of HTS cooling systems by forced convection: (a) LN2 subcooling with room-temperature core (Kyushu University, Japan), (b) helium gas cooling with core in vacuum (DOE SPI, USA) and (c) LN2 subcooling for core-and-coil assembly (Siemens, Germany).

$$Ra = \frac{g\beta \cdot \Delta T \cdot L^3}{\nu \cdot \alpha} \tag{2}$$

In Eq. (1), ν/α is the ratio of kinematic viscosity to thermal diffusivity (Prandtl number) of fluid, and H/L is

Table 1
Given parameters of 1 MVA transformer

Rating	Capacity, phase, frequency	1 MVA, 1ϕ, 60 Hz
	Voltage	22.9 kV/6.6 kV
	Current	44 A/152 A
Windings	Conductor	Bi-2223/Ag Tape (4.1×0.3 mm^2)
	Winding type	Double pancake (GFRP Bobbin)
	Number of turns	888/256
	Tape length	1248/1454 m
	Number of pancakes	8/4
	Outer/inner diameter	440/520 mm
	Height	450 mm
Core	Material	Silicon steel
	Diameter	270 mm
	Maximum field	1.7 T

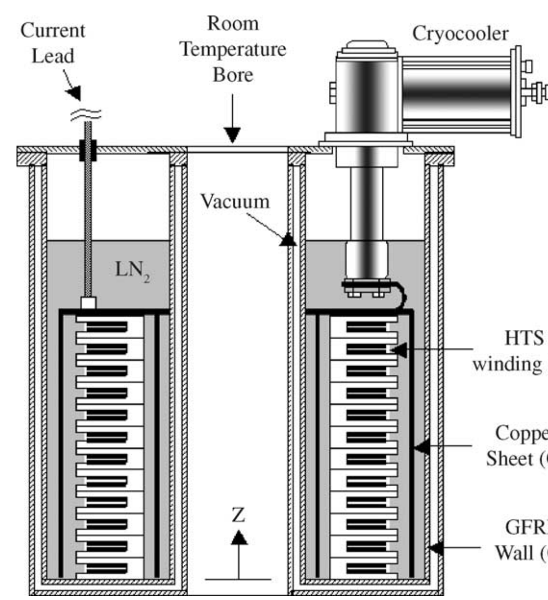

Fig. 2. Proposed design of cryogenic cooling system by natural convection of subcooled liquid nitrogen for Korean HTS transformer.

the aspect (height-to-length) ratio of the rectangular cavity. Fig. 4 is the plot of Nu as a function of Ra with various values of H/L, for liquid nitrogen at around 65 K. The Nusselt number increases as the Rayleigh number increases, because Ra is proportional to the ratio of the buoyancy to the viscous force, and the cellular flow near the walls becomes intensified (or even turbulent) at large values of Ra. On the other hand, the Nusselt number decreases as the aspect ratio increases, because the heat transfer on the heated wall is active at the bottom part and becomes less active along the ascending flow as the boundary layer grows, and the opposite is true on the cooled wall. For an infinitely large

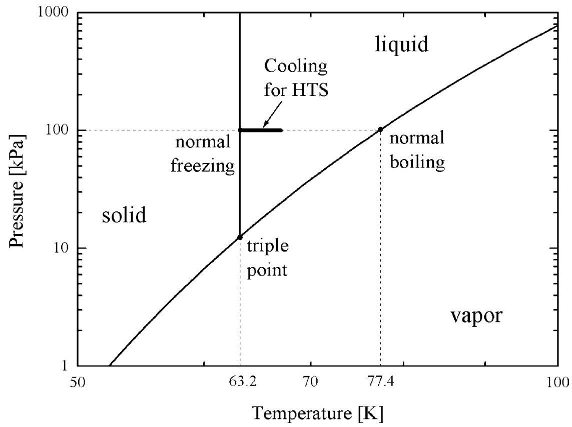

Fig. 3. Designed range of subcooled liquid on phase diagram of nitrogen.

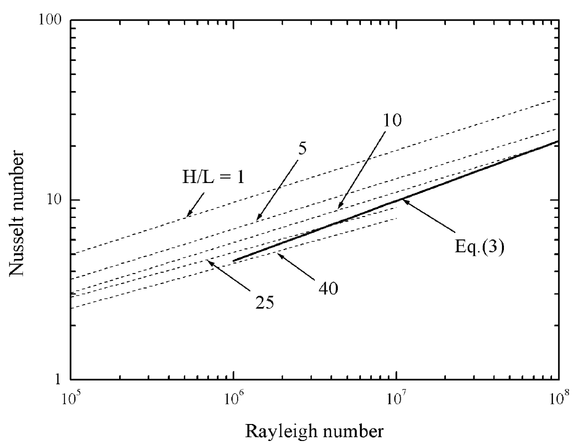

Fig. 4. Nusselt number for natural convection in vertical cavity.

aspect ratio, the velocity and temperature profiles are fully developed and the Nusselt number has its lower limit of $Nu = 1$.

The description in the previous paragraph is adequate in case that the surface temperature of each vertical wall is uniform. As the cryocooler is located above the windings in our proposed design, the main direction of heat flow is upward or the temperature should be lower at the top than at the bottom for all solid bodies including the HTS windings, the copper sheets, and the lower part of liquid-vessel walls. The natural convection between the vertical walls whose surface temperature decreases upwards could show a different behavior, as illustrated in Fig. 5. In case (a) that the vertical wall temperatures are uniform, a cellular flow could be formed in the cavity, as the ascending fluid is heated and the descending fluid is cooled along the streamline of flow. In case (b), however, that the vertical wall temperatures decrease upwards, the ascending fluid near the heating wall becomes warmer than the surface and the descending fluid near the cooling wall becomes cooler

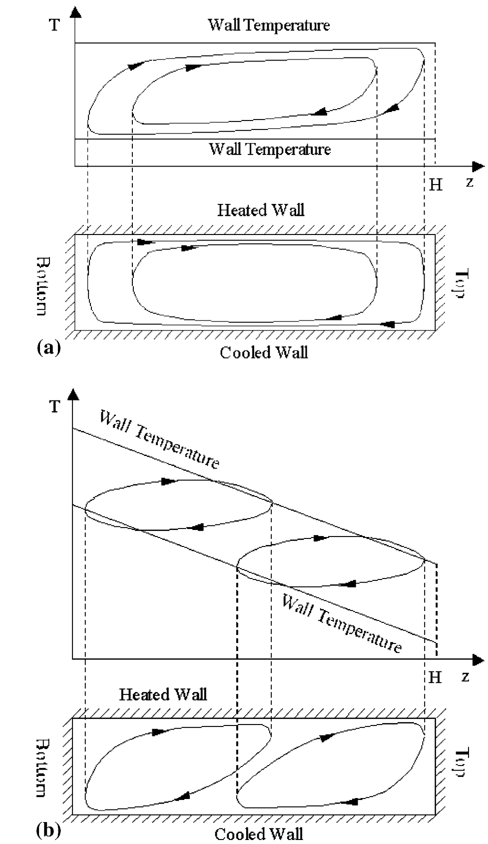

Fig. 5. Illustration of temperature along streamlines of natural convection: (a) surface temperatures uniform on vertical walls and (b) surface temperatures decreasing upwards on vertical walls.

than the surface the temperature, which may make the cellular flow vertically segregated. The number of cells may vary mainly by the temperature difference between the two surfaces and the vertical temperature gradient, but the flow must be multi-cellular if the bottom temperature of the cooled wall is higher than the top temperature of the heated temperature. The possibility of various flow patterns depending upon the thermal boundary conditions has been reported earlier [12,13].

An exact prediction of the heat transfer coefficient, therefore, does not seem to be easy in this specific situation. However, we would take one of the simplest empirical correlations [10,11]

$$Nu = 0.046 \cdot Ra^{1/3} \tag{3}$$

which is valid for $10^6 \leqslant Ra \leqslant 10^9$ and $1 < H/L < 40$. As plotted in Fig. 4, the Nusselt number from Eq. (3) may yield a slightly larger value than the other data, when $H/L > 25$ and $Ra \geqslant 10^6$. We expect that Eq. (3) should provide a good estimate in our problem (even for $H/L > 40$), because at least two segregated cells must be generated as discussed later and the effective aspect ratio is smaller than the actual H/L. It may be noted in Eq. (3) that the heat transfer coefficient, h, is independent of the horizontal distance between the walls, L, since Ra is proportional to L^3. In our design described below, the typical value of Ra is approximately 1.5×10^6 or $Nu \approx 5.3$.

3. Temperature distributions

There are two major sources of distributed thermal load to affect the temperature distribution of HTS windings; AC loss and thermal radiation. The AC loss is a dissipated heat in the HTS tapes of the windings and the thermal radiation is imposed from the room-temperature surface to the liquid-vessel wall. By taking into account the two distributed loads and the convection of liquid nitrogen, the steady-state temperature distribution in the HTS windings should be determined. The heat transfer problem is formulated into a set of differential equations, and then solved with both analytic and numerical methods for ensuring the correctness.

3.1. Formulation

A few simplifying assumptions are made for heat transfer analysis. First, the heat conduction in the solid bodies including the HTS windings, the copper sheets, and the liquid-vessel walls is one-dimensional in the vertical or axial direction. This assumption can be easily justified in this problem, because the thermal resistance for natural convection is dominant over the resistance for conduction in radial direction. Second, the AC loss and the heat transfer coefficient are uniform over the axial length. Even though the AC loss in HTS tape may be seriously affected by the perpendicular component of magnetic field [14–16], a spatially averaged value is used in this analysis. The temperature dependence of thermal conductivity is also neglected for a small temperature range. Third, the temperatures of inner and outer copper sheets are identical at the same axial position. This assumption on symmetry is valid, if the radial thickness of the pancake is much smaller than the diameter.

Upon these assumptions, the temperatures of the HTS windings (subscript H), the copper sheets (subscript C), and the liquid-vessel walls made of GFRP (subscript G) are determined by the three one-dimensional energy balance equations.

$$k_H A_H \frac{d^2 T_H}{dz^2} - h_{HC} P_{HC} (T_H - T_C) + \frac{Q_{ac}}{H} = 0 \tag{4}$$

$$k_C A_C \frac{d^2 T_C}{dz^2} + h_{HC} P_{HC} (T_H - T_C) + h_{GC} P_{GC} (T_G - T_C) = 0 \tag{5}$$

$$k_G A_G \frac{d^2 T_G}{dz^2} - h_{GC} P_{GC} (T_G - T_C) + Q'_r = 0 \tag{6}$$

In Eq. (4), the axial thermal conductivity of HTS pancakes, k_H, is estimated with the thermal resistance model for a composite conductor [17] and Q_{ac}/H is the average AC loss per unit axial length. Throughout this analysis, A, h and P denote the axial cross-sectional area, the heat transfer coefficient, and the perimeter of convection at an axial location, respectively. In Eq. (6), Q'_r is the radiation per unit axial length of wall, calculated by

$$Q'_r \approx \frac{\sigma P_G (300^4 - T_G^4)}{\frac{1-\varepsilon_G}{\varepsilon_G} + \frac{1}{F_{GR}} + \frac{1-\varepsilon_R}{\varepsilon_R}\frac{P_G}{P_R}} \approx \frac{\sigma P_G (300^4 - T_G^4)}{\frac{1}{\varepsilon_G} + \frac{1}{\varepsilon_R} - 1} \tag{7}$$

since both the radiation shape factor, F_{GR}, and the perimeter ratio, P_G/P_R, are nearly unity, so far as the gap (vacuum space) of the double-walled GFRP cryostat is much smaller than its diameter.

As the axial position, z, is measured from the bottom of the windings, the boundary conditions are given by

$$\frac{dT_H(0)}{dz} = \frac{dT_C(0)}{dz} = \frac{dT_G(0)}{dz} = 0 \tag{8}$$

$$k_H \frac{dT_H(H)}{dz} = h_c [T_H(H) - T_C(H)] \tag{9}$$

$$T_C(H) = 63.2 \text{ K} \tag{10}$$

$$\frac{dT_G(H)}{dz} = 0 \tag{11}$$

In Eq. (8), the radiation on the bottom plate of liquid-vessel is neglected, and Eq. (9) accounts for the mechanical contact at the top of the HTS pancake with the top copper plate which is maintained at the freezing temperature of nitrogen as given by Eq. (10). Eq. (11) means that the GFRP wall has a minimum temperature approximately at $z = H$, because the wall temperature should decrease upwards from the bottom to around $z = H$, but increase again above the point due to the heat conduction from the top plate at room temperature.

3.2. Approximate solution by integral method

The set of differential equations derived in the previous section is solved first by an integral method [18]. This analytical method is a well-known engineering technique to lead to an approximate solution that satisfies the global balance, as used in boundary layer problems. We start with integrating the governing equations, Eqs. (4)–(6), from $z = 0$ to H.

$$k_H A_H \frac{dT_H(H)}{dz} - h_{HC} P_{HC} \int_0^H (T_H - T_C)\, dz + Q_{ac} = 0 \tag{12}$$

$$k_{\mathrm{C}}A_{\mathrm{C}}\frac{\mathrm{d}T_{\mathrm{C}}(H)}{\mathrm{d}z}+h_{\mathrm{HC}}P_{\mathrm{HC}}\int_0^H(T_{\mathrm{H}}-T_{\mathrm{C}})\,\mathrm{d}z+h_{\mathrm{GC}}P_{\mathrm{GC}}\times\int_0^H(T_{\mathrm{G}}-T_{\mathrm{C}})\,\mathrm{d}z=0 \tag{13}$$

$$-h_{\mathrm{GC}}P_{\mathrm{GC}}\int_0^H(T_{\mathrm{G}}-T_{\mathrm{C}})\,\mathrm{d}z+Q_{\mathrm{r}}'H=0 \tag{14}$$

where the homogeneous boundary conditions, Eqs. (8) and (11), have been substituted. Eq. (14) means that all the radiation load should be transferred to the copper sheets by convection. Then Eqs. (13) and (14) are added to eliminate T_{G}.

$$k_{\mathrm{C}}A_{\mathrm{C}}\frac{\mathrm{d}T_{\mathrm{C}}(0)}{\mathrm{d}z}-h_{\mathrm{HC}}P_{\mathrm{HC}}\int_0^H(T_{\mathrm{H}}-T_{\mathrm{C}})\,\mathrm{d}z=Q_{\mathrm{r}}'H \tag{15}$$

At this point, we assume a simple functional form for $T_{\mathrm{H}}(z)$ and $T_{\mathrm{C}}(z)$ that can satisfy the boundary conditions. If parabolic functions

$$\frac{T_{\mathrm{H}}(z)-T_{\mathrm{H}}(H)}{T_{\mathrm{H}}(0)-T_{\mathrm{H}}(H)}=1-\left(\frac{z}{H}\right)^2 \tag{16}$$

$$\frac{T_{\mathrm{C}}(z)-T_{\mathrm{C}}(H)}{T_{\mathrm{C}}(0)-T_{\mathrm{C}}(H)}=1-\left(\frac{z}{H}\right)^2 \tag{17}$$

are taken for both temperature profiles, then

$$\frac{\mathrm{d}T_{\mathrm{H}}(H)}{\mathrm{d}z}=-\frac{2[T_{\mathrm{H}}(0)-T_{\mathrm{H}}(H)]}{H} \tag{18}$$

$$\frac{\mathrm{d}T_{\mathrm{C}}(H)}{\mathrm{d}z}=-\frac{2[T_{\mathrm{C}}(0)-T_{\mathrm{C}}(H)]}{H} \tag{19}$$

$$\int_0^H(T_{\mathrm{H}}-T_{\mathrm{C}})\,\mathrm{d}z=H\left\{\frac{2}{3}[T_{\mathrm{H}}(0)-T_{\mathrm{C}}(0)]+\frac{1}{3}[T_{\mathrm{H}}(H)-T_{\mathrm{C}}(H)]\right\} \tag{20}$$

By substituting Eqs. (18)–(20) into the derivatives and the integrals of Eqs. (9), (12) and (15), we have a set of three linear algebraic equations for $T_{\mathrm{H}}(0)$, $T_{\mathrm{C}}(0)$, and $T_{\mathrm{H}}(H)$, because $T_{\mathrm{C}}(H)$ is given by Eq. (10).

The most significant factor in designing the cryogenic cooling system is the temperature at the warm-end of the HTS pancakes. The temperature difference between $T_{\mathrm{H}}(0)$ and $T_{\mathrm{C}}(H)$ can be expressed in a closed form

$$T_{\mathrm{H}}(0)-T_{\mathrm{C}}(H)=\frac{H\left(1+\frac{2}{B}\right)\left[\left(1+\frac{3}{M}\right)Q_{\mathrm{ac}}+Q_{\mathrm{r}}'H\right]}{2\left[k_{\mathrm{H}}A_{\mathrm{H}}\left(1+\frac{3}{M}\right)+k_{\mathrm{C}}A_{\mathrm{C}}\left(1+\frac{3}{B}\right)\right]} \tag{21}$$

where two dimensionless parameters defined by

$$B=\frac{h_{\mathrm{c}}H}{k_{\mathrm{H}}}\quad M=\frac{h_{\mathrm{HC}}P_{\mathrm{HC}}H^2}{k_{\mathrm{C}}A_{\mathrm{C}}} \tag{22}$$

are concerned with the relative significance of thermal contact and the effectiveness of extended surface [10], respectively.

3.3. Numerical solution

In order to confirm the accuracy of the approximate solution by integral method, the same differential equations are solved by a numerical method. Since each differential equation is second-order and the two boundary conditions are imposed at two different ends, the numerical solution process should be an iterative one. The calculation starts by assuming three values of $T_{\mathrm{H}}(0)$, $T_{\mathrm{C}}(0)$, and $T_{\mathrm{G}}(0)$. As the axial temperature gradient at $z=0$ is given by Eq. (8), we numerically integrate Eqs. (4)–(6) from $z=0$ to H. At $z=H$, the calculated temperatures are checked for the three conditions, Eqs. (9)–(11). If these conditions are not satisfied, we take new values again for $T_{\mathrm{H}}(0)$, $T_{\mathrm{C}}(0)$, and $T_{\mathrm{G}}(0)$, and the same procedure is repeated until the agreement is attained. Fourth-order Runge–Kutta method is employed for numerical integration, and the shooting method by linear interpolation is used for improving the initial assumption.

4. Results and discussion

The temperature distributions calculated with the analytical and the numerical methods are compared in Fig. 6. The parameters in this specific calculation were taken from Tables 1 and 2. The analytical solution for liquid-vessel wall temperature is not plotted, as it is not uniquely determined by the integral method. The temperature of the HTS windings shows a noticeable amount of discrepancy in the middle of axial location, but an excellent agreement at the ends. The reason for these results is clearly that the analytical solution does not satisfy the local balance of energy, but does satisfy

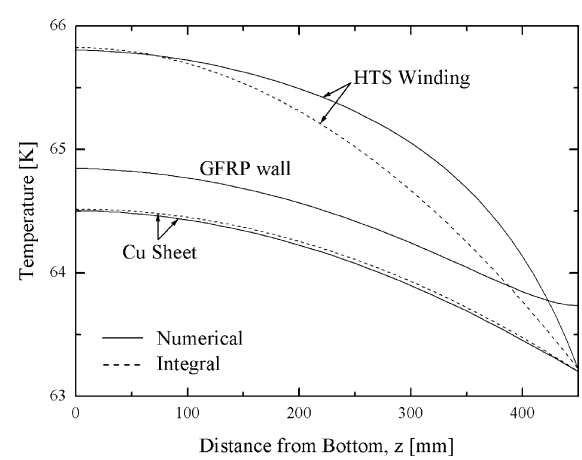

Fig. 6. Calculated wall temperature distributions from integral and numerical methods.

Table 2
Summary of cryogenic cooling design for 1 MVA transformer

Cryostat	Materials/insulation	GFRP/Vacuum and MLI
	Room temperature bore	300 mm
	Outer diameter/height	660 mm/950 mm
Copper sheets	Materials	Oxygen-free pure copper
	Thickness	10 mm
	Width/height	40 mm/450 mm
	Number of sheets	30 (Inside)/36 (Outside)
Operating temperatures	Cryocooler coldhead	60 K
	Top/bottom of windings	63.2 K/66 K
Cooling load	Conduction	17 W
	Radiation	39 W
	Current leads	18 W
	AC loss	83 W (55–138 W)
	Total	157 W (129–212 W)

the global balance. Since our major concern in cryogenic design is the warm end temperature of HTS windings, Eq. (21) can be evaluated as an accurate expression for the temperature with an accuracy of 99% or better in relevant conditions. It is also noted in Fig. 6 that the warm end temperature of copper sheets, $T_C(0)$, is higher than the cold end temperature of HTS wings, $T_H(H)$, which constitutes the condition for the multi-cellular flow in the cavity, as illustrated in Fig. 5(b).

Two main variables of the proposed design are the height of the HTS windings, H, and the thickness of copper sheets, δ_C, as the parameter, M, in Eq. (21) is given by

$$M \approx \frac{h_{HC}H^2}{k_C\delta_C} \tag{23}$$

The calculated warm-end temperature of HTS windings is plotted in Fig. 7, as a function of H and δ_C, when the other variables are the same as in Fig. 6. It is immediately obvious that as the thickness increases, the warm

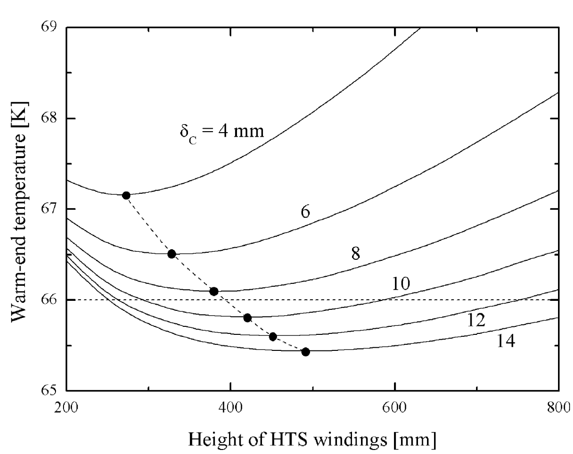

Fig. 7. Warm-end temperature of HTS windings as a function of winding height for various values of Cu sheet thickness.

end temperature decreases at any height of the windings. On the other hand, the effect of height on the temperature is more complicated. For a given thickness of copper sheets, there exists an optimum for the height to minimize the warm end temperature, as indicated by dots in Fig. 6. This behavior can be clearly explained with a simplified form of Eq. (21),

$$T_H(0) - T_C(H) \approx \frac{1}{2k_CA_C}\left[\left(H + \frac{3k_C\delta_C}{h_{HC}H}\right)Q_{ac} + H^2Q_r'\right] \tag{24}$$

which is valid in this situation, since $B \approx 500 \gg 1$ and $k_HA_H/k_CA_C \approx 0.01 \ll 1$. Among the three terms in the bracket of Eq. (24), the first and the third terms increase as H increases, because the AC loss becomes more widely distributed and more surface is exposed to the radiation. The second term, however, decreases, as H increases, which accounts for the effect of more surface area on the copper sheets. The optimal conditions are dependent upon the relative amount of the AC loss with respect to the thermal radiation. If the AC loss is dominant, the conditions are considerably reduced to $M = 3$ or $h_{HC}H^2 = 3k_C\delta_C$.

So far as these optimal conditions are satisfied and the design criterion is that the HTS temperature should not exceed 66 K (2.8 K above the freezing temperature of nitrogen), the proposed cooling by the natural convection may be feasible with the copper sheets whose thickness is approximately 9 mm or more, as shown in Fig. 7. The copper plates with this thickness should be acceptable for fabrication and joints. With a small safety factor, we take $H = 450$ mm and $\delta_C = 10$ mm for our immediate goal of 1 MVA transformer described in Table 1. It is also noted in Fig. 7 that the temperature criterion will be met for 300 mm $\leqslant H \leqslant$ 600 mm at $\delta_C = 10$ mm. If the height of HTS windings should be taller, the thickness of copper sheets may have to be greater, depending upon the design criterion of temperature. In order to avoid the eddy current, the copper sheets are split into many segments along the peripheral direction. The results of our cryogenic design are summarized in Table 2.

The most uncertain quantity in this analysis and design is the amount of AC loss in the HTS windings. The above calculations are based on 0.75 W/(kA m), in reference to the previous reports [1,2,14–16]. Since the dissipation is seriously affected by the direction of magnetic field, the actual AC loss may vary to a large extent with the winding design. There is also a good chance of additional dissipation at joints between the pancakes. Fig. 8 shows the effect of the AC loss on the warm end temperature for a fixed value at $\delta_C = 10$ mm. As the AC loss increases, the warm end temperature increases, but the optimal condition for the height of HTS windings does not vary significantly, because the AC loss is dominance in magnitude over the radiation.

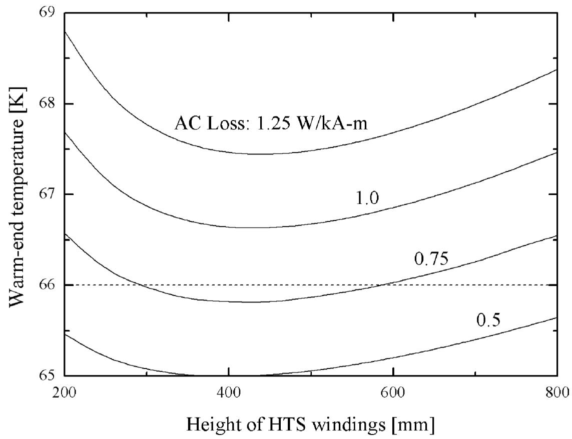

Fig. 8. Warm-end temperature of HTS windings as a function of winding height for various amount of AC loss.

Even though the AC loss may be different from the predicted value, the suggested cryogenic design for the physical dimensions does not need to be changed, which may be another nice feature of this cooling system. It is obvious, on the other hand, that the required thickness of copper sheets must be bigger if the AC loss is greater but the same temperature criterion is still applied.

5. Conclusions

A comprehensive heat transfer analysis is presented to evaluate our proposed design for the cryogenic cooling system of 1 MVA HTS transformer. It is rigorously shown that there exists an optimal condition for the height of the HTS windings, depending upon the amount of AC loss and the HTS-cryocooler interface. Under this condition, the proposed cooling system should be able to maintain the HTS windings only 2–3 K above the freezing temperature of nitrogen. We conclude that the cryogenic cooling by natural convection of subcooled liquid nitrogen is an excellent option for the prototype of HTS transformer, in all aspects of compactness, efficiency, and reliability. Further works are recommended, including an experimental verification of the proposed design and a scale-up study for larger capacity of HTS transformers.

Acknowledgements

This research is supported by a joint grant from the CAST (Center for Applied Superconductivity Technology) under the 21st Century Frontier R&D Program in Korea and the CAPS (Center for Advanced Power Systems) funded by the ONR (Office of Naval Research) Program in USA.

References

[1] Wolsky AM. Cooling for future power sector equipment incorporating ceramic superconductors. Argonne National Laboratory Report, The IEA Implementing Agreement for a Co-Operative Programme for Assessing the Impacts of High-Temperature Superconductivity on the Electric Power Sector. Argonne National Laboratory Report, April 2002. Available from: http://www.iea.org/tech/scond/scond.htm.

[2] Iwakuma M, Funaki K, Kajikawa K, Tanaka H, Bohno T, Tomioka A, et al. Ac loss properties of a 1 MVA single-phase HTS power transformer. IEEE Trans Appl Supercond 2001;11:1482–5.

[3] Funaki K, Iwakuma M, Kajikawa K, Hara M, Suehiro J, Ito T, et al. Development of a 22 kV/6.9kV single-phase model for a 3 MVA HTS power transformer. IEEE Trans Appl Supercond 2001;11:1578–81.

[4] Schwenterly SW, Cole MJ, Hazelton DW, Pleva EF. Performance of a prototype HTS power transformer cooling module. In: Applied Superconductivity Conference, August 2002, Paper #2LM04.

[5] Schlosser R, Schmidt HS, leghissa M, Meinert M. Development of high-temperature superconducting transformers for railway applications. In: Applied Superconductivity Conference, August 2002, Paper #2LM01.

[6] Kim WS, Hahn SY, Choi KD, Joo HG. Design of 1 MVA high T_c superconducting transformer. In: Applied Superconductivity Conference, August 2002, Paper #2LG01.

[7] Bladwin TL, Ykema JI, Allen CL, Langston JL. Design optimization of high-temperature superconducting power transformers. In: Applied Superconductivity Conference, August 2002, Paper #2LM07.

[8] Chang HM, Choi YS, Van Sciver SW. Optimization of operating temperature in cryocooled HTS magnets for compactness and efficiency. Cryogenics 2002;42:787–94.

[9] Chang HM, Choi YS, Van Sciver SW, Baldwin TL. Cryogenic cooling temperature of HTS transformers for compactness and efficiency. In: Applied Superconductivity Conference, August 2002, Paper #2LG04.

[10] Incropera FP, DeWitt DP. Fundamentals of heat and mass transfer. 3rd ed. New York: John Wiley & Sons; 1990.

[11] Barron RF. Cryogenic heat transfer. Philadelphia: Taylor & Francis; 1999.

[12] Ostrach S. Natural convection heat transfer in cavities and cells. In: Heat transfer—1982. Washington DC: Hemisphere Publishing; 1982. p. 365–79.

[13] Ho CJ, Lin YH. Natural convection of cold water in a vertical annulus with constant heat flux on the inner wall. J Heat Transfer 1990;112(2):117–23.

[14] Oomen MP, Haken B, Leghissa M, Rieger J. Optimum working temperature of power devices based on Bi-2223 superconductors. Supercond Sci Technol 2000;13:L19–24.

[15] Manusson N, Wolfbrandt A. AC losses in high-temperature superconducting tapes exposed to longitudinal magnetic fields. Cryogenics 2001;41(10):721–4.

[16] Fukuda Y, Toyota K, Kajikawa K, Iwakuma M, Funaki K. Field angle dependence of AC losses in stacked Bi-2223 Ag-sheathed tapes. In: Applied Superconductivity Conference, August 2002, Paper #4MC03.

[17] Chang HM, Kwon KB. Magnet/cryocooler integration for thermal stability in conduction-cooled systems. Adv Cryogenic Eng 2002;47:489–96.

[18] Arpaci VS. Conduction heat transfer. Reading, MA: Addison-Wesley; 1966.